Organic Process Research & Development **2004**, *8,* 998–1008

Application of Process Modelling Tools in the Scale-Up of Pharmaceutical Crystallisation Processes

Bernd Schmidt,* Jeegna Patel, Francois X. Ricard, Clemens M. Brechtelsbauer, and Norman Lewis
GlaxoSmithKline Pharmaceuticals, Old Powder Mills, Tonbridge, Kent, United Kingdom

Abstract:
Crystallisations are frequent process steps in the manufacture of active pharmaceutical ingredients (APIs). They are the primary means of intermediate or product formation and separation to achieve the desired purity and form. These unit operations are complex processes which are difficult to control due to the interlinked chemical and physical effects. For example, chemical aspects such as salt and polymorph concerns are in the forefront of process research, but physical effects manifesting themselves on scale-up, due to equipment influences, can be equally important for the successful outcome of a campaign. Several operational parameters, such as temperature or impeller speed, need to be understood and controlled to achieve constant desupersaturation, consistent narrow particle size distribution around the desired mean, minimal attrition, and homogeneous growth conditions. This paper focuses on the equipment influence on crystallisations, relating it to first principles with respect to heat and momentum transfer, analysing it with computational fluid dynamics (CFD), and demonstrating its process impact using examples from recent development work. Dynamic process modelling and CFD are state-of-the-art engineering tools to identify process requirements and match them with equipment capabilities. The work reported here demonstrates how a semiquantitative application of these tools can lead to a controllable, robust process in an existing plant despite the time and resource limitations usually encountered in the industry.

1. Introduction

The scale-up of crystallisation processes represents one of the most complex tasks in process engineering as usually a number of target quantities have to be kept within narrow boundaries, such as yield, selectivity, purity, and often particle size distribution. In the pharmaceutical industry this complexity is enhanced further as only small amounts of APIs are usually available in early stages of development. This limits the number and scale of experiments significantly and, in fact, prevents thorough process investigations at an intermediate pilot scale. Furthermore, pilot plant and manufacturing vessels can often not be characterised prior to a manufacturing campaign due to time and resource constraints. The process chemist or engineer has therefore only a minimum of information available to achieve a "right-first-time" process scale-up. A method to compensate for this constraint is the use of computational engineering tools based on CFD and dynamic process modelling.

* Corresponding author. E-mail: bernd.2.schmidt@gsk.com.

The development of methods related to these tools, including the numerical solution of differential equations, goes back as far as the late 1950s and early 1960s with work by Collatz[1] and Harlow et al..[2,3] Despite the availability of these methods for the past 40 years, the application of CFD and dynamic process modelling software was limited to users who then had access to highly sophisticated and very expensive computer equipment, mainly to be found in military and aviation research. Only in the past fifteen years or so, due to great advances in microprocessor technology, enough calculating power at reasonable cost had been made available to a wider user base. This, in consequence, has created a market for a number of companies providing CFD and process modelling software and has extended the application to further fields of commercial interest, including the flow and reaction profile within stirred tank reactors in the chemical and pharmaceutical industry. Since then, the use of CFD and process modelling tools has steadily increased, from simulating simple single phase flows and reaction kinetics to assessing multiphase systems with complex kinetic profiles.

This paper presents two case studies on how the combination of these computational modelling tools and experimental methods at laboratory scale can result in a robust scale-up of a pharmaceutical crystallisation process in a relatively short time using a minimum of resources.

2. Theoretical Background

Chemical aspects, such as solubility and polymorphism,[4] play a key role in the initial design of a crystallisation process. Achieving the correct crystal morphology is one of the main goals of a crystallisation process design. The second main goal is to deliver a robust process scale-up from laboratory to pilot plant and manufacturing scale to minimise variability in product quality between batches. To achieve this, it is essential to understand the chemistry and related information such as solubility and kinetics.

During scale-up, however, physical effects can become equally important for the success of a campaign as the underlying chemistry itself, which is shown in the two case studies below. For example, particle size and the particle size distribution (PSD) can be influenced through settling, attrition, agglomeration, and local flow conditions. These

(1) Collatz, L. *The Numerical Treatment of Differential Equations*, 3rd ed.; Springer: Berlin, 1960.
(2) Harlow, F. H.; Dickman, D. O.; Harris, D. E.; Martin, R. E. *Two-Dimensional Hydrodynamic Calculations*; Los Alamos National Laboratory Report LA-2301, 1959.
(3) Harlow, F. H.; Meixner, B. D. *The Particle-And-Force Method for Fluid Dynamics*; Los Alamos National Laboratory Report LA-MS-2567, 1961.
(4) Laird, T. *Org. Process Res. Dev.* **2003**, *7*, 957.

Published on Web 11/04/2004
10.1021/op040013n CCC: $27.50

effects are based on parameters directly linked to the concept of mixing, such as power input per unit volume, suspension, shear, and heat transfer, all of which can be investigated using CFD software and which must be considered on scale-up.

Such an investigation, however, only leads to qualitative or, combined with integral scale-up rules and experimental investigations, to semiquantitative results. To achieve a fully quantitative scale-up, intrinsic kinetic data have to be collected and correlated with the reactor setup and geometry via CFD software. However, this method is very time, material, and resource intensive and relies on the ready availability of full experimental data sets. Especially in the fine chemical and pharmaceutical industry, this desirable situation is far from reality as there are often severe constraints in these areas.

Therefore, a method is presented on how these limitations can be overcome by applying a semiquantitative approach based on the combination of experimental work, the application of integral scale-up rules and CFD/process modelling tools and, last but not least, process experience.

2.1. Physical Aspects. For the successful application of scale-up rules based on the four mixing concepts of power input per unit volume (P/V), suspension, shear and heat transfer, it is important to ensure geometrical similarity between the crystallisation vessels, including impellers and baffles, from laboratory to pilot and manufacturing plant[5] scale. Each of these quantities requires a different scale-up criterion depending on stirrer speed, and ideally, all of them should be kept constant on scale-up. However, keeping one criterion constant always violates another. For example, a certain stirrer speed, determined by maintaining the suspension conditions constant on scale-up, might be ideal to suspend particles in a specific process at large scale but might at the same time lead to crystal attrition due to an increase in tip speed. This would then lead to the creation of fines with adverse effects on downstream processing, such as filtration. It is, consequently, important to perform laboratory experiments to determine the main influencing parameters and associated scale-up factors. CFD models can then be applied to verify the obtained experimental and calculated results of a projected process scale-up.

2.1.1. Power Input per Unit Volume. A widely recommended scale-up criterion is the power input per unit volume P/V (W m^{-3}) or the correlated energy dissipation rate ϵ (W kg^{-1}).[6−8]

$$\frac{P}{V} = \frac{P_o \rho N^3 D^5}{V} \tag{1}$$

$$\epsilon = \frac{P}{m} = \frac{P_o \rho N^3 D^5}{m} \tag{2}$$

Depending on the process, the integral value of power input over the bulk or local values can be governing factors in the achievement of the desired output. Especially in the case of micromixing controlled antisolvent precipitations,[9,10] local values of the power input are likely to be dominant as the crystal formation is localised to the point of antisolvent addition. For macromixing controlled crystallisations or precipitations, the integral value of P/V or the mixing time θ have to be kept constant on scale-up.[11] High values for both local and integral P/V could lead to the creation of too many fines, low values to large crystals with inclusions.

2.1.2. Suspension. To achieve homogeneous crystal growth, all particles need to be suspended in the mother liquor to provide the maximum possible surface area and, consequently, homogeneous conditions regarding the mass transfer from the liquid to the solid phase. Zwietering[12] defined the "just-suspension-speed" N_{js} as the minimum impeller speed at which no particle remains static at the vessel base for more than 1 to 2 s.

$$N_{js} = s\nu^{0.1}(g\Delta\rho/\rho_L)^{0.45}X^{0.13}d_p^{0.2}D^{-0.85} \tag{3}$$

The resulting criterion of $N_{js} \cdot D^{0.85} =$ constant still is one of the main criteria used in the scale-up of crystallisation processes. If not all crystals are fully suspended, a widening of the particle size distribution (PSD) can be expected as well as particle agglomeration and encrustation at the vessel base. An impeller speed above N_{js} does not show any significant mass transfer benefits[13] but is often used to ensure that the crystals are not "just suspended" but homogeneously distributed within the bulk. To achieve homogeneity in the degree of suspension, N_{js} is often multiplied with a safety factor in the region 1.2 to 1.5.

2.1.3. Shear. The habit of crystallized pharmaceutical products is often far from the "ideal" sphere. Frequently, APIs can crystallize in the form of needles, which are susceptible to breakage. This can lead to the creation of fines with adverse consequences regarding downstream process steps such as filtration and may also result in secondary nucleation which can seriously affect the particle size distribution of the final product. If this effect needs to be avoided or if the PSD of shear sensitive crystals needs to be kept within narrow boundaries, the shear rate at the impeller blade tip, where its value is at a maximum, must be considered. Therefore, the tip speed u should be kept constant on scale-up.

$$u = N\pi D \tag{4}$$

However, the average shear rate decreases in response to the speed, which may explain why one often attains a shift of the PSD to higher values upon scale-up,[14] i.e., tip speed is a conservative scale-up criterion.

2.1.4. Heat Transfer. In the case of cooling crystallisations, it is important to ensure homogeneous heat transfer conditions at the internal vessel wall in order to avoid the formation of local wall temperature gradients. This concept

(5) Zlokarnik, M. *Scale-up in Chemical Engineering*; Wiley-VCH: June 2002.
(6) Krebs; Forschner. *DECHEMA Kolloquium Mixing of Fluids*; Frankfurt, 1993.
(7) Geisler, R. K.; Buurman, C.; Mersmann, A. B. *Chem. Eng. J.* **1993**, *51*, 29−39.
(8) Todtenhaupt, E. K.; Zeiler, G. *Handbook of Mixing Technology*; Ekato: Germany, 2000.
(9) Mersmann, A.; Kind, M. *Chem. Eng. Technol.* **1988**, *11*, 264−276.
(10) Zauner, R.; Jones, A. G. *Chem. Eng. Sci.* **2002**, *57*, 821−831.
(11) Baldyga, J.; Bourne, J. R. *Turbulent Mixing and Chemical Reactions*; Wiley: England, 1999.
(12) Zwietering, T. N. *Chem. Eng. Sci.* **1958**, *8*, 244−253.
(13) Nienow, A. W.; Miles, D. *Chem. Eng. J.* **1978**, *15*, 13−24.
(14) Genck, W. J. *www.cepmagazine.org*. June 2003; pp 36−44.

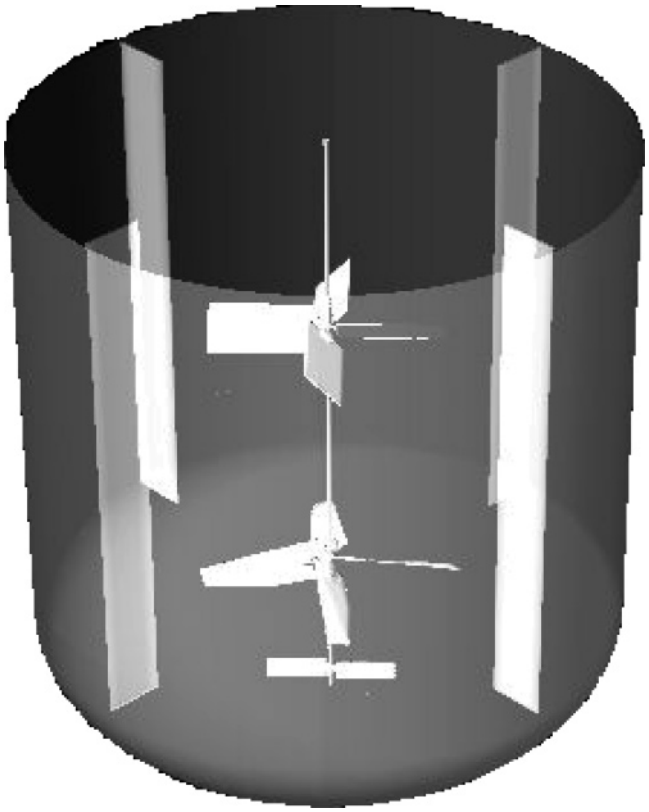

Figure 1. **Single-phase model geometry setup in CFX-ProMixus_2.1 using information specified in Table 1.**

can lead to wall encrustation or to an inhomogeneous desupersaturation profile within the bulk, consequently widening the resulting particle size distribution. The investigation of heat transfer in the context of crystallisation processes can be performed using CFD to obtain qualitative information on the wall shear profile on the internal vessel wall, which is discussed in the first case study. This concept is derived from the following Reynold's analogy:

$$\frac{q_o}{\rho C_p \frac{dT}{dy}} = \frac{\tau_o}{\rho \frac{du}{dy}} \tag{5}$$

which states, in effect, that the rate of energy transport normal to the wall bears the same relation to the energy gradient as the shear stress bears to the momentum gradient.[15]

To assess the influence of a vessel's heat transfer capability on a cooling crystallisation process, the volume related heat flux

$$\frac{dQ_v}{dt} = U_v V \Delta T \tag{6}$$

and the heat capacity C_p of the bulk should be taken into account rather than just the heat transfer at the vessel wall, as the ratio of heat transfer area to reaction volume decreases significantly on scale-up, leading to a less efficient overall heat transfer.

2.2. CFD Modelling. CFD is a versatile tool which can be used to assess mixing processes in a wide range of geometrical configurations, thereby reducing requirements for experiments at laboratory and plant scale. Figure 1 displays a geometry which was investigated in CFX-ProMixus_2.1 Express[16] using the CFX-TASCFlow solver (Table 1 describes the model setup data). The express option of the software automatically sets up and performs a three-dimensional hexahedral element-based finite-volume, quasi-transient,[17] multiple-frame-of-reference (MFR) CFD analysis.[18] Here, the wall shear profile was investigated to detect hot/cold regions in the vessel (Figure 2). Warmer colours indicate a high shear rate; zones of good heat transfer at the wall can be observed around the impeller region, whereas the liquid surface is cooler. Detecting hot/cold regions is particularly important for cooling crystallisations when it is imperative to have controlled desupersaturation.

High shear zones can also be identified to provide an understanding of where the crystals might be damaged and

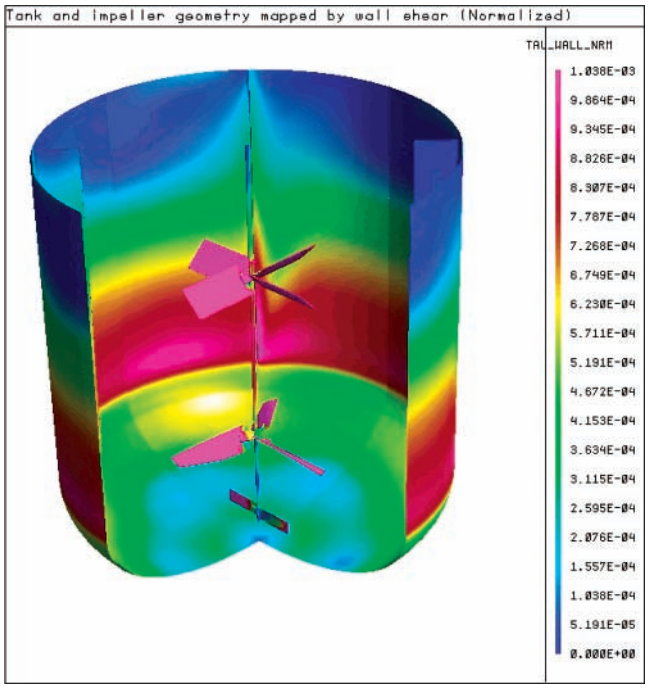

Figure 2. **Wall shear profile from CFX-ProMixus_2.1 model using geometrical information specified in Figure 1 and Table 1.**

Table 1. **CFX-ProMixus_2.1 single-phase model data**

tank geometry	dish based vessel
tank diameter	1.8 m
fluid level	1.547 m
number of impellers	3
rotational speed	90 rpm
impeller 1 type	four-bladed 45° pitched blade turbine pumping downward
impeller 1 diameter	0.7 m
impeller 1 clearance	1.23 m
impeller 2 type	3 bladed 39° hydrofoil pumping downward
impeller 2 diameter	0.8 m
impeller 2 clearance	0. 43 m
impeller 3 type	two-bladed flat blade turbine
impeller 3 diameter	0.4 m
impeller 3 clearance	0.015 m
no. of baffles	4
type of baffle	flat baffles
baffle offset	0.019 m
baffle width/depth	0.18 m/1.547 m

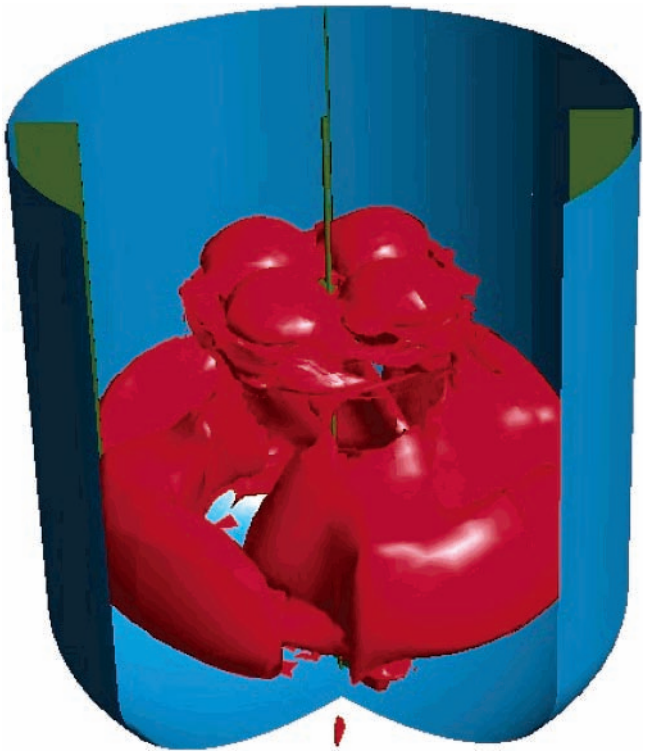

Figure 3. **High shear fluid zone from CFX-ProMixus_2.1 model using geometrical information specified in Figure 1 and Table 1.**

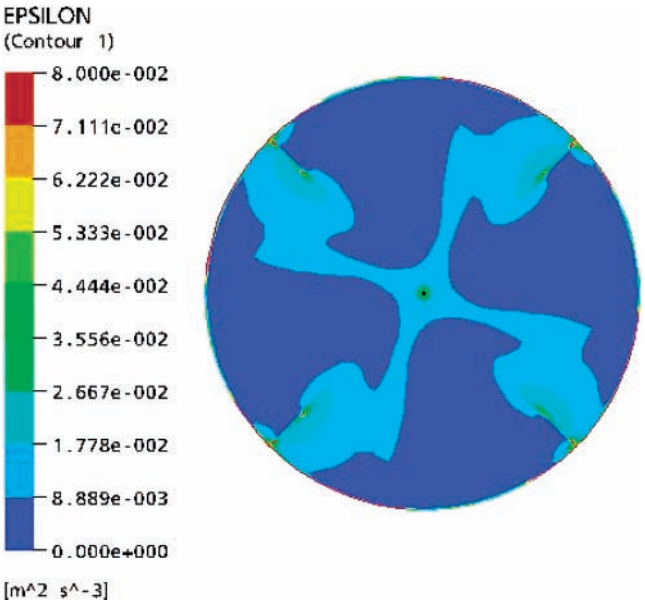

Figure 4. **Local energy input at liquid surface from CFX-ProMixus_2.1 model using geometrical information specified in Figure 1 and Table 1.**

secondary nucleation occurs. Figure 3 shows such a plot. For this particular geometry at the specified operating conditions, the highest shear zones were around the impeller region.

For crystallisations involving antisolvent additions, the local energy input can be plotted from which the ideal point of addition can be identified. Figure 4 displays such information at the liquid surface; for this particular geometry, the highest local energy input can be found in the region of the baffles, indicating good local micromixing. This would therefore be the recommended point of addition.

During the first case study, the CFD code Fluent 6.0 in combination with MixSim 2.0 (Fluent Inc., USA) was used. During the second case study, the CFD code CFX 4.4 (ANSYS Inc., USA) was used. It is possible to run simulations using both MFR and sliding mesh.[17] However, since sliding mesh is computationally very demanding, all models were run using MFR analysis. Single-phase models were run as steady-state, and once a converged solution was achieved, the analysis was changed to unsteady-state for multiphase modelling. Assumptions made during the modelling will be discussed in more detail in section 3.

Overall, these CFD capabilities can be used to quickly and economically assess a process, as only a minimum level of information is required.

2.3. Crystallisation Kinetics. To predict the performance of a batch cooling crystallisation on scale-up, the kinetics of the crystallisation process have to be determined to quantify any potential impact on product yield. Several models for the determination of batch crystallisation kinetics have been suggested, most of which take into account crystal growth and nucleation to predict the PSD.[19−22] However, due to severe time and resource limitations in the second case study, PSD aspects were decoupled from the kinetic equation for a separate investigation using CFD.

Therefore, a desupersaturation model based on a first-order mass transfer was used,

$$r = k'A_s(c_{eq} - c) = k'\alpha V_s(c_{eq} - c) = kV_s(c_{eq} - c) \qquad (7)$$

which describes the rate of product transfer from the liquid to the solid phase in a sequence of discrete time steps. This model assumes that all the material, which is transported to the solid phase due to desupersaturation, is deposited on the crystal surface. To solve this equation it is necessary to measure the intrinsic mass transfer rate during desupersaturation [dN/dt], determine the equilibrium saturation, c_{eq}, by measuring the solubility curve of the investigated system and calculating the total solid-phase volume, V_s. The kinetic constant k' can be combined with the specific surface area α to the kinetic parameter k (eq 7), if identical seed material is used in the experimental study as well as in the scaled-up process. k can then be determined by fitting the experimental kinetic data using commercial software such as, e.g., DYNOCHEM (Performance Fluid Dynamics Ltd., Ireland).

3. Case Studies: Description

When scaling up single or multiphase processes, it is important to ensure geometrical similarity between the labora-

(15) Rannie, W. D. Heat transfer in turbulent shear flow, Thesis, California, 1951.
(16) *CFX-ProMixus_2.1 Manual*; AEA Technology plc, 2000.
(17) Versteeg, H. K.; Malalasekera, W. *An Introduction to Computational Fluid Dynamics: The Finite Volume Method*; Pearson Higher Education: August 1995.
(18) Luo, J. Y.; Issa, R. I.; Gosman, A. D. *IChemE*, Symp. Series. 136; September, 1994; pp 549−556.
(19) Mullin, J. W.; Nyvlt, J. Programmed Cooling of Batch Crystallizers. *Chem. Eng. Sci.* **2001**, *26*, 369−377.
(20) Randolph, A. D.; Larson, M. A. *Theory of Particulate Processes*, 2nd ed.; Academic Press: New York, 1988; p 369.
(21) Zhou, Y.; Kovenklioglu, S. *Chem. Eng. Commun.* **2004**, *191*, 749−766.
(22) Monnier, O.; Fevotte, G.; Hoff, C.; Klein, J. P. *Chem. Eng. Sci*. **1997**, *52*, 1125−1139.

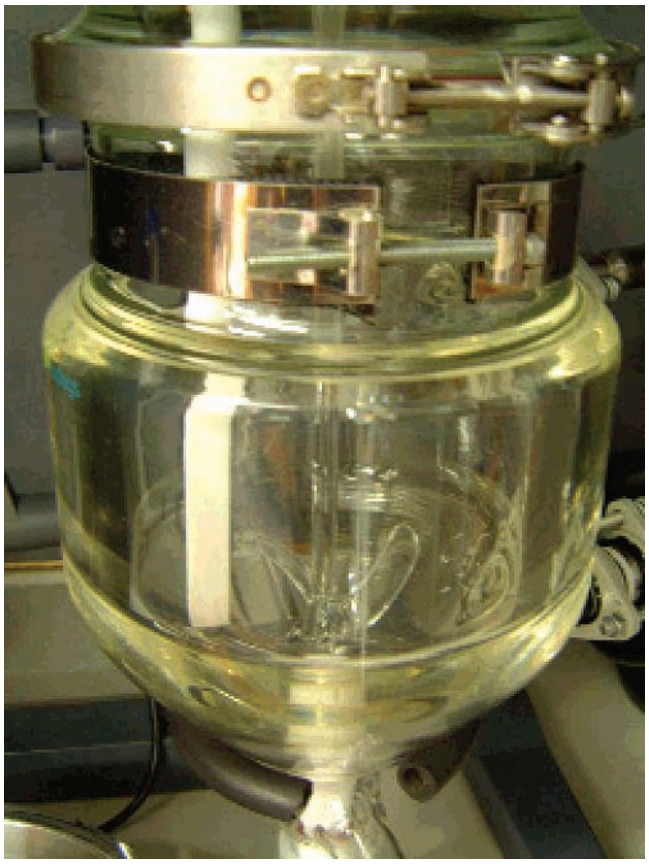

Figure 5. **Experimental setup used for scale-down studies for both compounds B and S; 2 L conical based CLR fitted with a retreat curved impeller (90 mm diameter) angled at 45° to the vertical and a beavertail-shaped baffle of 15 mm diameter.**

tory scale vessels, used for experimental investigations, and pilot plant or manufacturing scale vessels. In the case of the two presented examples, the cooling crystallisation of an organic API, B, and the crystallisation of a compound, S, both processes were to be scaled up into conical base reactors at pilot plant scale (50 L for compound B and approximately 250 L for compound S) and manufacturing scale (approximately 630 L for compound S).

The experimental investigations were carried out in a 2 L conical base glass reactor with a heat transfer jacket. Heating and cooling were provided by synthetic oil (HUBER DW-Therm) circulating through a "HUBER Unistat Tango" heat exchange unit (Peter Huber Kaeltemaschinenbau GmbH, Germany). Figure 5 shows the experimental setup, including a PTFE beavertail baffle and a Retreat Curved impeller, RCI, powered by an IKA stirrer motor (IKA Werke GmbH & Co. KG, Germany). The 2 L scale was used as it is a good compromise between the minimum scale at which scale effects can be observed and the already mentioned, and often severe, material constraints.

Conical base reactors are widely used in the pharmaceutical industry to serve multiple applications, e.g., as crystallisation vessels. Despite the wide use of this type of vessel, little has been done so far to improve understanding of its hydrodynamic characteristics. This is reflected in the near absence of relevant publications. Although the reactor geometry is not ideal for suspending solids, these are the constraints of employing a multipurpose plant. Therefore the term "homogeneous suspension" in this paper indicates a condition at which an increase in stirrer speed would not significantly change the solids distribution inside the solvent mixture; it does not refer to a fully homogenised solids distribution profile in the bulk liquid.

In both case studies, the key physical parameters, which were degree of suspension, shear sensitivity, and heat transfer, were selected and investigated in more detail. This selection was driven by the type of process and observations from previous experimental work, where shear and suspension appeared to have an effect. CFD contributed a major part in investigating these physical parameters and providing essential qualitative information for scale-up.

3.1. First Case Study. In this example, the final seeded cooling crystallisation stage of a process to produce the API B will be discussed. The key aim of this study was to have a reproducible, narrow particle size distribution for this step due to the downstream processing requirements, i.e., filtration and drying, as well as subsequent micronisation of the final drug substance. This could be achieved by (1) providing homogeneous growth conditions to promote particle uniformity, (2) ensuring low shear to prevent attrition, and (3) having good heat transfer to ensure a constant and controlled desupersaturation.

Transfer of this process was planned from 2 L lab scale to 50 L pilot plant scale, to provide material for pharmaceutical development. To initially assess the process in the pilot scale vessel, CFD modelling provided qualitative information. The CFD code Fluent 6.0, in combination with MixSim 2.0, was used. Since it was important to ensure controlled desupersaturation, the heat transfer at the vessel wall was of interest. Therefore, a wall shear profile was plotted to detect hot and cold regions in the vessel. From observations of previous experimental work, suspension was considered an important parameter, in particular to avoid encrustation at the vessel base. Shear was also deemed an important parameter for this process due to the crystal morphology (rosettes which were susceptible to breakage). CFD was used to initially gather such data, i.e., determining high shear zones and obtaining solid distribution plots. To initially assess the process, several assumptions were made on the process physical properties required for the model as listed below:

- spherical particles
- all particles of same diameter (50 μm) and density
- Eulerian nongranular model assumed applicable
- run at just suspension speed, calculated from Zwietering correlation (equation 3)

The crystal density had previously been measured to 1.4 g cm^{-3}.

Preliminary results obtained were sufficient to ascertain whether the geometrical configuration was suitable for maintaining good crystal suspension and providing the required shear characteristics. However, for this process, where degree of suspension and shear have been previously observed to have an effect on particle size and crystal size distribution, such influences cannot be quantitatively predicted through CFD. A scale-down study in the geometrically

similar 2 L vessel was, therefore, required to quantify these effects and also to appreciate how the process behaved in such a geometrical configuration. To gather the necessary information with a minimum number of experiments, three experiments were selected. The first was conducted at the homogeneous suspension speed, the second, at high shear, and the third, at just suspension speed, experiment two and three being the worst case scenarios. It should be noted that seed loading, quality, and PSD were not considered during the experimental work, as the same input material was used for the pilot scale batches.

The overall heat transfer coefficient, U_a, of the lab scale vessel was of the same order as the pilot scale vessel (200−500 W m^{-2} K^{-1}), therefore the same heating and cooling times used in the pilot plant vessel were applied. All other parameters remained constant during the three experiments. The final product was dried in a vacuum oven to minimise attrition. Malvern sizing[23] was performed on the final dried material retrieved from all experiments to obtain the particle size distributions.

To verify the predictions, the CFD model for the 50 L pilot scale vessel was updated with the calculated impeller speed.

3.2. Second Case Study. The crystallisation process with respect to S is a product recrystallisation and consists of a seeded evaporative crystallisation followed by a cooling crystallisation step from a temperature of approximately 70 °C to 20 °C to maximize the total process yield. The amount of material added for recrystallisation is approximately 6% w/w, and the amount of seed material, approximately 0.03% w/w of the total input. The main goals of this study were

(1) to ensure a consistent product yield of approximately 90% w/w on scale-up,

(2) to establish homogeneous crystal growth conditions within the pilot plant scale reactor of 250 L volume, and

(3) to transfer this process information into a 630 L manufacturing vessel.

Further, the qualitative influence of suspension and shear on the PSD was investigated. Therefore laboratory experiments, using a 2 L conical base reactor with the same geometrical setup as the pilot plant and manufacturing vessel, were conducted. N_{js} was determined in water, a solvent with low product solubility, using a typical product material with an average particle size of approximately 190 μm. The crystallisation process was then investigated at laboratory scale at three different impeller speeds, (i) below N_{js}, (ii) at N_{js}, and (iii) at an impeller speed which was 30% above the minimum stirrer speed to achieve homogeneous suspension and investigate the influence of increased shear. The reaction parameters and the experimental results were used to build a CFD multiphase model using the software CFX 4.4. The crystals of this process are bipyramids, but to simplify the CFD model, a spherical shape with a measured crystal density of 1.4 g/cm^3 was assumed. Scale-up correlations based on the experimental results were used to determine the required impeller speed in the 250 L pilot vessel, a total scale-up factor of 125 from the 2 L laboratory vessel. To compensate for this relatively large factor and the small number of laboratory experiments due to a lack in starting material, simulations based on the CFX 4.4 model, now using the plant geometries, were used to verify the calculated stirrer speed. The information of the laboratory experiments together with the results of the successful pilot plant campaign delivered the required information for a scale-up from 250 L into the 630 L manufacturing vessel. The same methodology as for the scale-up from the 2 L into the pilot scale vessel was applied.

For an assessment of the potential impact of a less effective heat transfer on the bulk temperature profile and the product yield on scale-up, a DYNOCHEM process model was generated. It comprised a kinetic model, based on a first-order mass transfer, the system inherent solubility curve, and a heat transfer model based on a volume related heat flux.

As the seed material used in this kinetic study was identical to the one to be used during the pilot plant and manufacturing campaign, the rate constant k' and the specific crystal surface area α were combined to the kinetic parameter k.

To determine k, a seeded crystallisation experiment was conducted at 100 mL scale to measure the rate of desupersaturation at two different temperatures, 28 °C and 59 °C, within the cooling crystallisation temperature range using ATR-UV.[24] The experiments were conducted at a stirrer speed of approximately 1000 rpm to avoid any influence of the stirrer speed on the desupersaturation profile. The solubility curve for compound S in the solvent mixture, to obtain c_{eq} as a function of temperature, was measured using the same analytical technique.

The process model, consisting of the fully descriptive rate equation and the volumetric heat transfer model, was verified by simulating the cooling profile applied in 2 L scale laboratory experiments. The U_v value of the vessel was measured to approximately 3 kW m^{-3} K^{-1} before carrying out the experimental work. The imposed jacket temperature profile consisted of a cooling period of approximately 1.5 h followed by an aging period of approximately 1 h. The same jacket temperature profile was simulated for the process at 250 L pilot and 630 L manufacturing scale with estimated U_v values of 2 kW m^{-3} K^{-1} and 1.5 kW m^{-3} K^{-1}, respectively, to assess whether the desired bulk temperature profile and, hence, yield could be achieved. These U_v values were based on an estimated U_a value[25] of 200 W m^{-2} K^{-1}, which is typical for these vessel sizes.

4. Case Studies − Results and Discussion

4.1. First Case Study. A wall shear profile of the 50 L pilot plant vessel was plotted to detect hot and cold spots (Figure 6). Zones of good heat transfer at the wall can be observed around the region of the impeller, whereas the surface is cooler. Figure 7 shows the particle size analysis results obtained from the lab experiments which were

(23) Rawle, A. *Basic Principles of Particle Size Analysis*; www.malvern.co.uk, printed April 2004.

(24) Urban, M. W. *Attenuated Total Reflectance Spectroscopy of Polymers: Theory and Practice (Polymer Surfaces & Interfaces S.)*; American Chemical Society: 1996.

(25) Perry, R. H.; Green, D. W. *Perry's Chemical Engineers' Handbook*, 7th ed.; McGraw-Hill: New York, 1997.

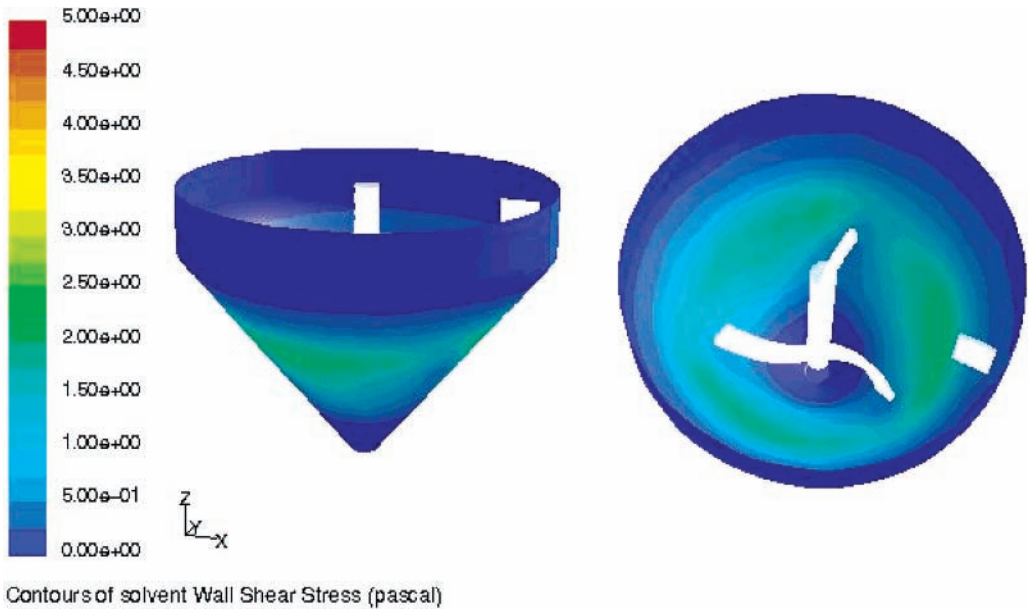

Figure 6. **Wall shear plot from preliminary CFD model of compound B.**

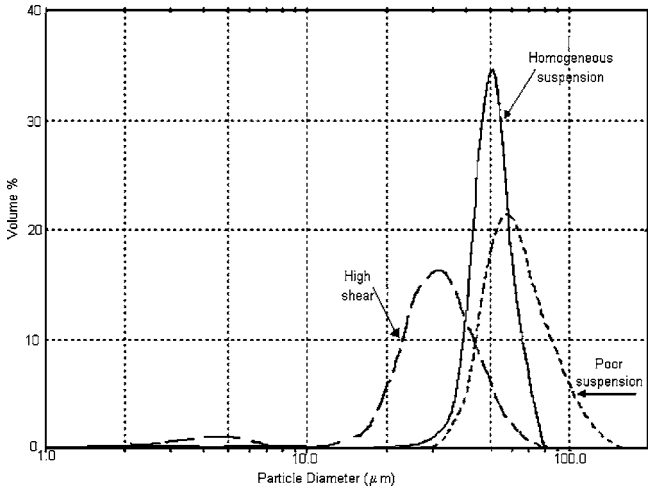

Figure 7. **Particle size analysis results from laboratory experiments for compound B: plot of volume % of particles versus corresponding particle diameter.**

conducted (1) at homogeneous suspension speed (310 rpm), (2) at a high shear (450 rpm), and (3) at just suspension speed N_{js} (250 rpm). When the crystals were poorly suspended at N_{js}, a wide particle size distribution was observed maybe due to the presence of agglomerates and large variations in shear. It has to be noted that, due to the dispersed Malvern sizing method, it was not possible to determine the presence of agglomerates. When the crystals appeared to be homogeneously suspended, a narrower particle size distribution was obtained with a lower average particle size, which can be explained by the improved growth conditions and the overall increased average shear rate. High shear conditions resulted in a wider particle size distribution, which was bimodal with yet a lower average particle size. The increase in maximum shear rate resulted in smaller particles overall. The bimodal distribution was due to the considerable increase in tip speed (15%) causing the creation of more fines, as a higher volume fraction of crystals were in the high shear region of the impeller. Therefore, the experimental conditions

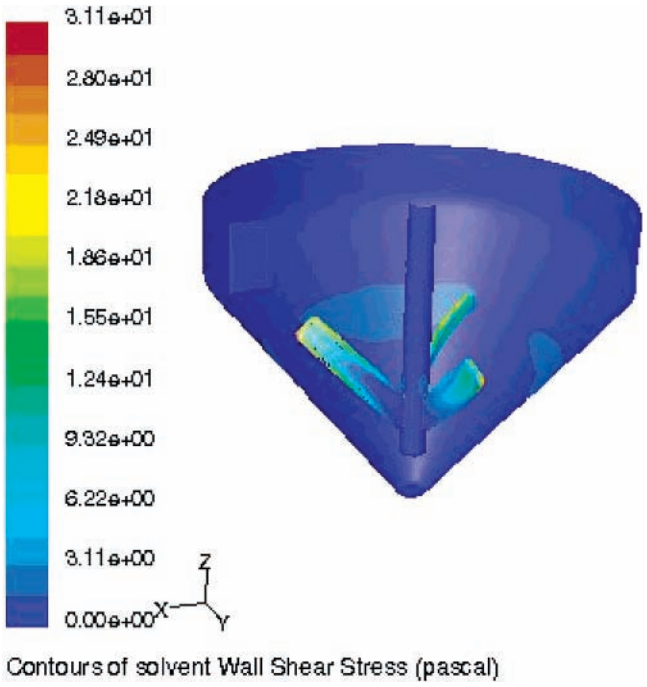

Figure 8. **Wall shear profile of PP vessel using modified model of compound B.**

correlated well with the results, showing that experiment 2 and 3 with high shear and poor suspension resulted in undesirable particle size distributions.

Using observations and results of the laboratory experiments, the narrowest particle size distribution was achieved with homogeneous suspension conditions. Therefore, this parameter was considered the most important. Since constant geometrical similarity was maintained from the investigated 2 L laboratory scale to the 50 L pilot plant scale, and the physical properties were the same, the following was derived from the Zwietering correlation:

$$N_{lab}D_{lab}^{0.85} = N_{plant}D_{plant}^{0.85} \quad (8)$$

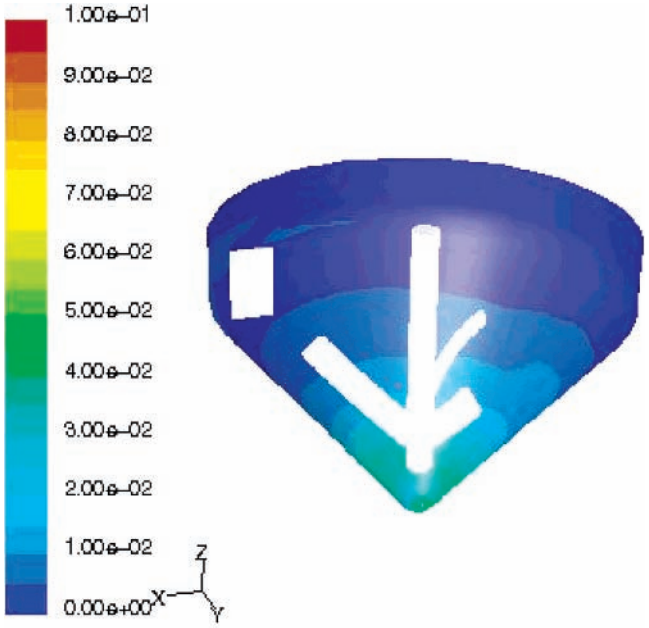

Figure 9. **Solid distribution results of PP vessel using modified model.**

Table 2. **PSD analysis results of the 2 L scale experiments of the second case study**

experiment ref. no.	d_{10} [μm]	d_{50} [μm]	d_{90} [μm]
(i) below N_{js} (150 rpm)	73	233	443
(ii) at N_{js} (300 rpm)	88	198	299
(iii) homogeneous suspension speed (390 rpm)	51	158	280

This equation was used to calculate the speed required to homogeneously suspend the crystals in the 50 L pilot scale vessel, which was found to be 120 rpm.

Finally, shear profiles were plotted to determine the zones with the highest shear rate and, hence, highest attrition (Figure 8). It can be observed that there is a higher degree of attrition at the impeller blade tips where the shear rate is at a maximum. The shear profile at the wall is reasonably homogeneous, therefore reducing the risk of creating hot and cold regions. The solids distribution plots (Figure 9) confirm that, at the recommended impeller speed, the crystals are well suspended, although there is a slightly higher concentration of solids swirling at the vessel base (less than 5% of the entire volume), since it is difficult to achieve complete homogeneous distribution of solids in this type of vessel. With these geometrical configurations, i.e., a conical based vessel fitted with a radial flow impeller and lack of adequate baffling, solids will tend to swirl around the conical base. Even at elevated impeller speeds, it is difficult to achieve complete homogeneity due to the poor top to bottom mixing. Although the recommended impeller speed results in an increase in maximum shear rate of 17%, there is a reduction in the average shear rate of 23%.

Following a structured procedure, sufficient data were gathered for understanding the physical aspects affecting this particular crystallisation using a minimum amount of material and maximizing the use of CFD. Pilot plant results showed that, at the recommended impeller speed, no settling occurred, the crystals were well suspended, and the average particle size, d_{50}, was 53 μm, which was comparable to the lab scale (d_{50} of 50 μm at 310 rpm).

4.2. Second Case Study. The 2 L lab scale experiment to determine N_{js}, using product material in water, delivered a value of 300 rpm. The crystallisation experiment conducted at the same impeller speed delivered an average particle size d_{50} of 198 μm. A subsequent qualitative mixing study to assess the impact of poor suspension and high shear on the crystal size was carried out at 150 and 390 rpm, respectively. The analysis of the particles confirmed that, due to most of the crystals not being suspended at 150 rpm, the average particle size increased to 233 μm, and a widening of the particle size distribution of more than 80% compared to the experiment at 300 rpm could be observed. The experiment at 390 rpm resulted in a d_{50} of 158 μm and a similar relative PSD width as that at 300 rpm, confirming the break-up of crystals as a consequence of the higher shear stress at the impeller tip (Figure 10). The presence of agglomerates could

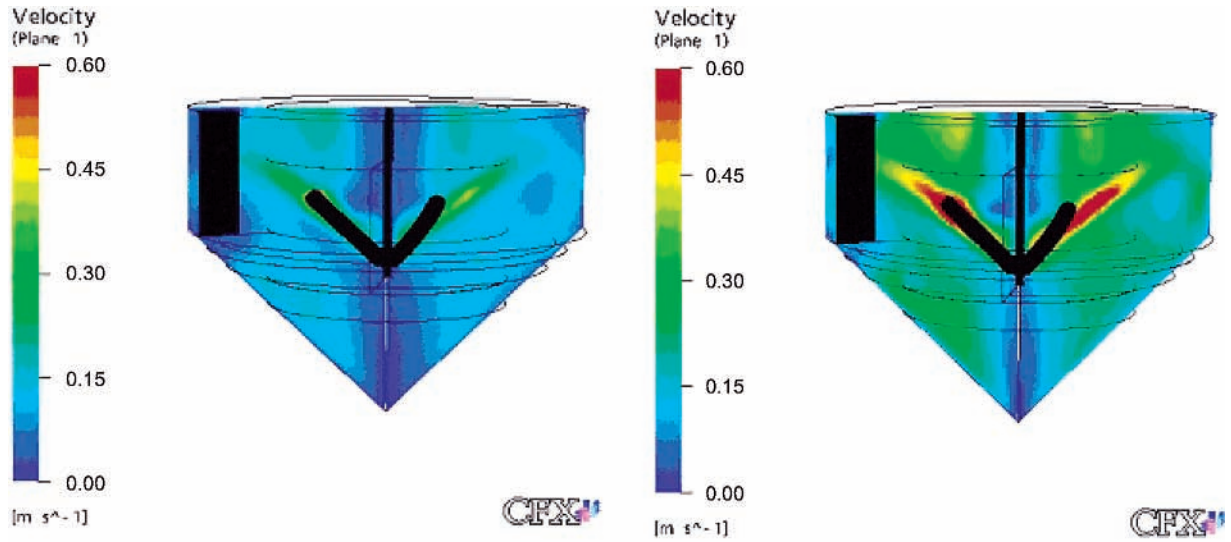

Figure 10. **Velocity plot for compound S in 2 L CLR at (a) 300 rpm and (b) 390 rpm.**

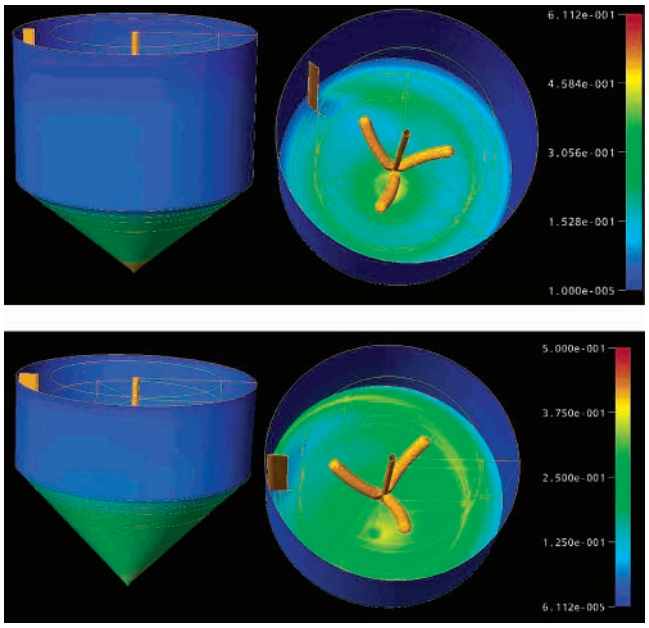

Figure 11. **Solids distribution of S in 250 L and 630 L reactor.**

be excluded following microscopic analysis. Table 2 shows the PSD analysis results of the three 2 L scale experiments.

Based on eq 8 and a safety factor of 1.3, the calculated impeller speed at 250 L scale was determined to be 105 rpm. This speed ensured the required homogeneous suspension conditions during the pilot plant campaign and resulted in a d_{50} of approximately 195 μm. For the 630 L scale manufacturing vessel, a stirrer speed of 85 rpm could be determined based on a constant impeller tip speed (eq 9) derived from eq 4, which delivered a d_{50} of approximately 250 μm.

$$N_{\text{lab}}D_{\text{lab}} = N_{\text{plant}}D_{\text{plant}} \tag{9}$$

An explanation for the observed shift in PSD from 250 L to 630 L scale is the already mentioned decrease in the average shear rate,[11] which in this case could be determined to approximately 27%. The multiphase CFD models for the 250 L and the 630 L vessel at 105 and 85 rpm (Figure 11) show similar solids distributions, as volume fraction of solids, in the 250 L and the 630 L vessel, respectively. A significant accumulation of the crystals at the vessel base on scale-up cannot be observed, which verifies the integral scale-up correlations applied in this case.

To determine the kinetic parameter k of the fully quantitative process model, the kinetic equation (eq 7) was fitted to the experimentally acquired data, which delivered a value of 3 s^{-1}. Figure 12 shows the measured as well as the fitted desupersaturation profiles at 28 °C and 59 °C. Temperature did not seem to have an influence on the rate of desupersaturation in the investigated temperature range, and a wall shear assessment using CFX ProMixus_2.1, as already discussed in the first case study, confirmed the absence of hot and cold spots in the laboratory as well as in the pilot plant and manufacturing vessel. Figure 13 shows the measured solubility curve. The data were approximated using an exponential function, which was entered into the process model to represent the solubility data in a simple mathematical term.

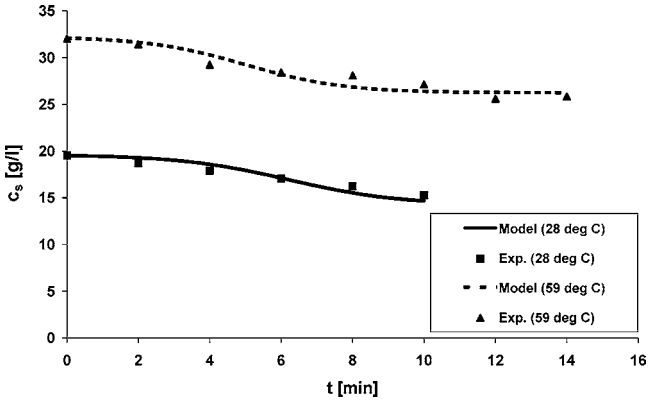

Figure 12. **Desupersaturation of S over time: model and experiment (ATR-UV).**

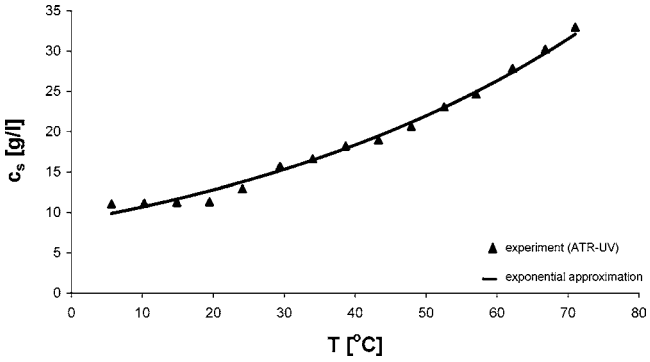

Figure 13. **Solubility curve of compound S.**

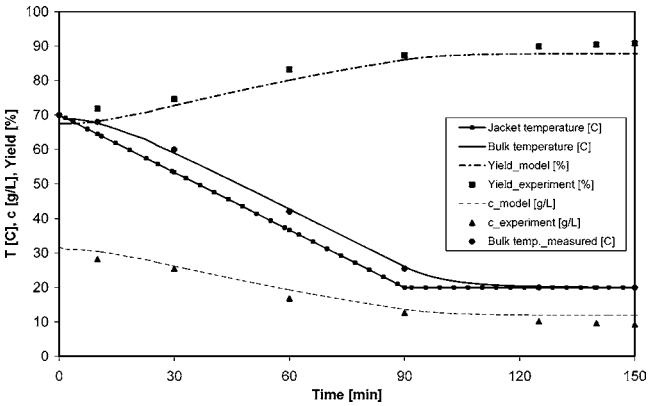

Figure 14. **Simulation of a typical crystallisation of compound S at 2 L laboratory scale (U_v = 3 kW m^{-3} K^{-1}).**

The 2 L experiment, to verify the predictive process model, delivered a yield of 90% w/w. A process simulation was run using the same parameters as those in the experiment. A jacket temperature profile of a 90 min cooling time from 70 °C to 20 °C followed by a 60 min aging time at 20 °C was entered into the model, as was the fill level and the amount of seed and dissolved product material. Figure 14 shows the simulated as well as the experimentally acquired temperature, concentration, and yield profiles. The simulated product concentration in solution, c_model, the derived product yield, Yield_model (in % w/w), and the temperature of the solution, bulk temperature (in °C), over time correlate well with the experimental values (c_experiment, Yield_experiment, and Bulk temp._measured). The slight difference be-

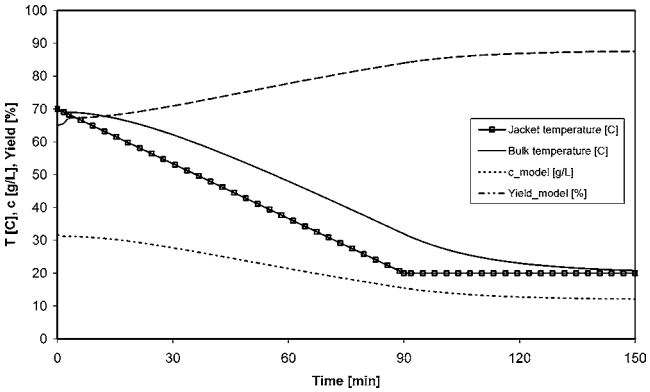

Figure 15. **Simulation of the pilot plant campaign at 250 L scale with an estimated U_v of 1.5 kW m^{-3} K^{-1}**

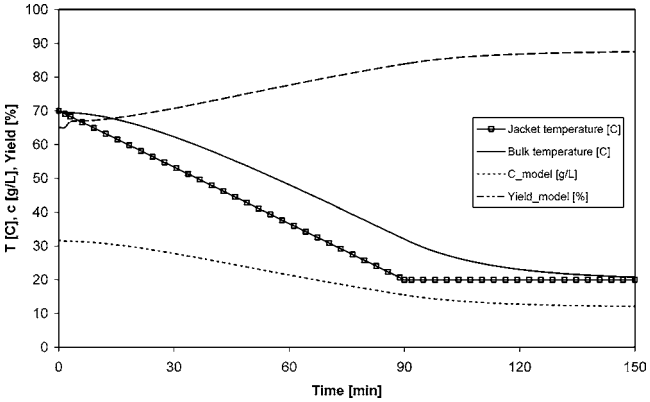

Figure 16. **Simulation of the manufacturing campaign at 630 L scale with an estimated U_v of 1.5 kW m^{-3} K^{-1}.**

tween the simulated and the measured product concentration in solution can be explained by the crude exponential approximation of the solubility curve in the process model. Further, the kinetic model does not take into account the order of the crystallisation process, which is likely to be different from 1. An approach based on the model suggested by Mullin and Nyvlt[19] should produce a more accurate prediction.

Figures 15 and 16 show the results of the process simulation for the 250 L pilot plant and the 630 L manufacturing vessel. In both cases, a yield loss on scale-up can be excluded, as the imposed cooling profile results in the required final bulk temperature of approximately 20 °C to maximize the product yield. The pilot plant as well as the manufacturing campaign were conducted at the initially planned cooling profile and produced both yields above 90% w/w.

5. Conclusions

There are several complex phenomena associated with crystallisation processes which need to be taken into account. Ideally, all physical aspects should be considered, for example, kinetics of the crystallisation, heat transfer characteristics of the vessel, degree of crystal suspension, and shear profile in the vessel, to appreciate the underlying phenomena and ensure a successful process. However, to consider these aspects would require significant time, material, and manpower. Using existing information on process behaviour, the type of crystallisation process, and crystal properties, the most relevant to the process can be selected and investigated in more detail. The two examples discussed in this paper demonstrate the significance of applying these concepts for understanding process behaviour. Modelling tools are used to minimise material requirements, generate qualitative information, and verify other means of scale-up predictions.

Application of these methodologies results in understanding the complex processes behind crystallisations and gathering relevant data for scale-up in a short amount of time.

Acknowledgment

We gratefully acknowledge the analytical support from Duncan Thompson, Lesley Senior, Wendy Cross, Philip Lake, and Zoe Ford. Further, we thank Steve Coote, Dean Edney, John Seager, Hardev Singh, Andrew Kennedy, Roz Nice, and Tracy Lee-Ching Koh for providing valuable process information. Received for review May 21, 2004.

Nomenclature

b	order of nucleation
c	concentration, mol m^{-3}
c_{eq}	equilibrium saturation, mol m^{-3}
C_p	specific heat capacity, kJ kg^{-1} K^{-1}
D	impeller diameter, m
d_p	particle diameter, μm
d_{10}	10% of the particles are less than this particle diameter, on volume basis, μm
d_{50}	50% of the particles are less than this particle, on volume basis, μm
d_{90}	90% of the particles are less than this particle, on volume basis, μm
dT/dy	temperature gradient normal to wall, K m^{-1}
du/dy	velocity gradient normal to wall, s^{-1} m^{-1}
g	gravitational acceleration, m s^{-2}
k	kinetic parameter, s^{-1}
k'	kinetic constant, m s^{-1}
m	mass, kg
N	impeller speed, rpm
N_{js}	just suspension speed, rpm
P	power, W
P_o	power number
q_o	heat flow rate per unit area normal to wall, W m^{-2}
Q_v	heat output, J
r	rate of desupersaturation, mol s^{-1}
s	constant in Zwietering equation
t	time, s
u	tip speed, m s^{-1}
u	velocity at the wall, m s^{-1}
U_a	overall heat transfer coefficient at vessel wall, W m^{-2} K^{-1}
U_v	overall volumetric heat transfer coefficient, W m^{-3} K^{-1}
V	volume, m^3
V_s	solid volume, m^3

α	specific surface area, m^{-1}
ϵ	energy dissipation rate, W kg^{-1}
ν	kinematic viscosity, m^2 s^{-1}
θ	mixing time, s
μ	dynamic viscosity, Pa s
ρ	density, kg m^{-3}
ρ_l	liquid density, kg m^{-3}
$\Delta\rho$	liquid density − solid density, kg m^{-3}
τ_o	shear stress at wall, N m^{-2}

Abbreviations

API	active pharmaceutical ingredient
ATR-UV	attenuated total reflection ultraviolet sensor
B	organic compound B − API
CFD	computational fluid dynamics
CLR	controlled laboratory reactor
CSD	crystal size distribution
eq	equation
MFR	multiple-frames-of-reference
P/*V*	power per unit volume
PSD	particle size distribution
PTFE	polytetrafluorethylene
RPS	rotations per second
Re	Reynolds number ($= \rho ND^2/\mu$)
RCI	retreat curved impeller
S	organic compound S − API

Received for review May 21, 2004

OP040013N